The Role of High Rydberg States in the Generation of Negative Ions in Negative-ion Discharges

J.R. Hiskes

This paper was prepared for submittal to

International Symposium of Negative Ion Production
Brookhaven, New York
October 23-27, 1995

November 28, 1995

Lawrence
Livermore
National
Laboratory

DISCLAIMER

THE ROLE OF HIGH RYDBERG STATES IN THE GENERATION OF NEGATIVE IONS IN NEGATIVE-ION DISCHARGES

J. R. Hiskes
Lawrence Livermore National Laboratory

ABSTRACT

The presence of high Rydberg states in a negative-ion discharge will increase the concentration of negative ions on the order of order of one per cent compared to those generated via dissociative attachment to ground-state vibrationally-excited molecules.

INTRODUCTION

The generation of substantial yields of H^- ions in a laser excited H_2 gas has been reported by Pinnaduwage and Christoforu.[1,2]

These H^- yields have been attributed to (2+1) REMP photoexcitation processes leading to dissociative attachment of doubly-excited or superexcited states (SES), or dissociative attachment of high Rydberg product states. The new feature of these experiments is the implied large dissociative attachment rates, of order $10^{-6} cm^3 sec^{-1}$, values that are orders-of-magnitude larger than the dissociative attachment of the vibrationally excited levels of the ground electronic state.

While these laser excitations are not directly applicable to a hydrogen negative-ion discharge, the implication of large dissociative attachment rates to the high Rydberg states may affect both the total negative-ion density and the interpretation of discharge performance. Within the discharge energetic electrons will collisionally excite the higher Rydberg states, and the relative contribution of the dissociative attachment of these states when compared with the dissociative attachment to the ground state vibrational levels, is the topic of this paper.

GENERATION OF THE RYDBERG POPULATION DENSITY

The rate equation for the excitation of an electronic state N_R of the H_2 molecule is

$$d N_R(n)/dt = n_f N_2 \, \sigma v(1-n) - N(n)\left\{n_f\left[\sigma v(i)+\sigma v(e)\right]+n_{th}\left[\sigma v(DA)+\sigma v(e)\right]+A_n\right\} \quad (1A)$$

where $N(n)$, N_2, n_f and n_{th} are the densities of the excited electronic states with principal quantum number parentage n, gas density, fast electron density and thermal electron density; the $\sigma v(1-n)$ is the electron excitation rate from the ground state to level n, $\sigma v(i)$, $\sigma v(e)$, $\sigma v)DA)$ are the ionization, excitation, and dissociative attachment rates, and A_n the radiative decay rate. For the equilibrium solution, $dN/dt=0$, one has

$$N_R(n) = n_f N_2 \, \sigma v(1-n)\left\{n_f\left[\sigma v(i)+\sigma v(e)\right]+n_{th}\left[\sigma v(DA)+\sigma v(e)+\sigma v(i)\right]+A_n\right\}^{-1} \quad (1B)$$

Here the solutions of Eqs.1A, 1B will be compared with the discharge data of Eenshuistra et al.[3]

The princi;al excitations are to the $^1\Sigma_g$, $^1\Sigma_u$, and $^1\Pi_u$ states. For states $n < 7, 8$, the radiative term, A_n, dominates in the bracket. The equilibrium solution of Eq (1) becomes

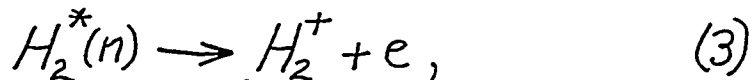$$N_R(n) = n_f N_2 \, \sigma v(1-n) A_n^{-1}. \quad (2A)$$

The excitation rates as a function of parentage quantum number, n, are plotted in Fig. 1 for each of the sequences

$$n p\sigma \, ^1\Sigma_u, \quad n p\pi \, ^1\Pi_u, \quad and \quad n s\sigma \, ^1\Sigma_g$$

and for incident electron energies of 40 eV. There is experimental data for states through n= 4; for the higher Rydberg states these cross sections are extrapolated as n^{-3}.

The radiative transition probabilities, A_n, are plotted in Fig. 2. Again, the transition probabilities beyond n=3 are scaled as n^{-3}. The $^1\Sigma_g$ states are somewhat ambiguous. The E, F$^1\Sigma_g$ state has an anomolously small transition probability, since only the lower lying B$^1\Sigma_u$ state is accessible by radiative decay. For higher $^1\Sigma_g$ states both $^1\Sigma_u$ and $^1\Pi_u$ states are accessible by radiative decay in analogy with the atomic transitions. For the $n s\sigma \, ^1\Sigma_g$ states higher than the E, F state the equivalent atomic transition probabilities are used.

Electronic states with Rydberg parentage equal to n=3 or higher ($D'\Pi_u 3p\pi$ and higher states) are subject to internal conversion which in the case of the H_2 molecule manifests itself through autoionization,

$$H_2^*(n) \longrightarrow H_2^+ + e, \tag{3}$$

provided the vibrational level, v, of the state in question lies above the ground vibrational state of the H_2^+ ion. For these Rydberg states the internuclear potential functions closely approximate that of the H_2^+ ion, and the vibrational population fractions, $f(v)$, calculated for the ionization of H_2 to form H_2^+ [4], can be used to approximate the $H_2^*(v)$ populations.

The fraction of Rydberg excitations, F(n) that survives autoionization is

$$F(n) = \sum_v f(v), \tag{4}$$

where the upper limit on v is the highest level that lies below the v=o level of H_2^+. This limit is obtained by inspection of Sharp's diagram [5]. The values for F(n) are given in Table I. The $'\Sigma_g$ values are taken equal to the $'\Sigma_u$ values.

TABLE I

n	State	F(n)
2	$B\,'\Sigma_u$	1.
	$C\,'\Pi_u$	1.
3	$B'\,'\Sigma_u$	1.
	$D\,'\Pi_u$	.84
4	$B''\,'\Sigma_u$	.68
	$D'\,'\Pi_u$	.57
5	$B'''\,'\Sigma_u$	.41
	$D''\,'\Pi_u$	.41
6	$B''''\,'\Sigma_u$	.25
	$D'''\,'\Pi_u$	.25
7	$B'''''\,'\Sigma_u$	.09
	$D''''\,'\Pi_u$	.09

States n=7 and higher have only their ground vibrational level lying below the ground level of H_2^+ ,and for these states all F(n)=.09. The σv(1−n) in Eq. 2A is replaced with F(n)σv (1−n).

Above the state n=7 the collisional-radiative process is changed in a qualitative way. The radiative decay of the n=7 state is offset by the larger collisional excitation rate to n=8 state. These Δn =1 excitations increase as n^4, specifically

$$\sigma\,(n, n+1) = \sigma_o\, n^4, \qquad (5)$$

with σ_o= 3 x 10^{-16} cm^2. The rapid increase of this collision processes at successively higher states causes a runaway cascade terminated by ionization at the highest bound state sustainable in the discharge environment.

The steady-state rate equations for an array of states beginning at n=7 is solved taking into account the array of collision processes given by (5) and

$$\sigma\,(n+1, n) = \sigma_o\, n^4 . \qquad (6)$$

From these solutions one obtains

$$N_R\,(7+k)/N_R(7) = \left(\frac{1}{2}\right)^k, \qquad k = 1,2,3,.... \quad (7)$$

i.e., the n=8 level has one-half the population of n=7, the n=9 level one-fourth the population, etc.

One can sum the populations of all states above n=7,

$$\frac{1}{N_R(7)} \sum_{k=1}^{\infty} N_R\,(7+k) = \sum_{k=1}^{\infty} \left(\frac{1}{2}\right)^k = 1, \qquad (8)$$

that is to say the entire population above n=7 equals the population of the n=7 state.

The cross sections for excitation of the triplet states at 40 eV are only five to fifteen percent of the singlet excitations, but with comparable radiative transition probabilities. An exception is the $2 p\pi c\, {}^3\Pi_u$ state with A=10^4 sec^{-1} . This state is collisionally excited to the rapidly decaying and close lying $a\, {}^3\Sigma_g$ state in a time $\simeq 8$ μsec to give an effective transition probability $A\,({}^3\Pi_u) \simeq 1.2 \times 10^6 s^{-1}$

The solutions for the Rydberg populations, $N_R(n)$ mol. cm^{-3}, are obtained from Eqs. 1 and plotted in Fig. 3. Here we have increased the populations by ten percent to account for the triplet excitations.

These population distributions are shown in two approximations: In the lower limit case only the population of the n=7 state originating from the $\sigma(1-7)$ excitation is included in the upward cascade. In the upper limit all higher excitations given by the sum $\sum_{k=1}^{\infty} \sigma(1 \rightarrow k)$ are included for excitations initiated at the n=7 level.

GENERATION OF THE NEGATIVE ION DENSITY

The negative ion density generated by each Rydberg state is given by

$$N_R^-(n) = n_{th} N_R(n) \sigma v (DA) \{ n_{th} [\sigma v (CD + \sigma v (ii)] + N_i \sigma v (AD) \}^{-1} [1 - e^{-D\bar{t}}], \quad (9)$$

where the successive collision terms in the denominator, D, are electron collisional detachment, ion-ion neutralization, and associative detachment by collisions with atoms, N_i. The total negative ion concentration is

$$N^- = \sum_{n=1}^{\infty} N_R(n). \qquad (10)$$

In Fig. 4 are plotted the negative ion concentrations as a function of discharge electron temperature taken from the FOM experiment.[3] The error bars have been reported by Hopman.[7]

At the previous Symposium in this series the author reported[8] the calculation of the ion density at kT=1.4eV, using the numerical negative ion code and assuming dissociative attachment to the vibrational levels, $H_2(v)$, belonging to the ground state. In this earlier calculation only those solutions for the $H_2(v)$ that fell within the experimentally observed range were retained for the calculation of the negative ion density. The result of this calculation at $kT = 1.4 eV$ is shown by the ~~diamond~~ *triangle* on the figure. These calculations have now been extended to the lower electron temperatures and fall within the range of the experimental uncertainties.

Ignoring the ground state $H_2(v)$ contributions but including the Rydberg contribution given by Eq. 10, the upper and lower limit calculations are shown on the lower part of the figure. Comparing, the $H_2(v)$ contribution to the negative ion density is approximately fifty times larger than the Rydberg contribution.

The group at the Wright Laboratories[10] have also performed calculations for the negative ion density including only contributions from the Rydberg states and taking into account only the collisional excitation, $\sigma(1-n)$, and the subsequent radiative decay. Their solutions are shown by the circles in Fig. 4, and are seen to be approximately a factor of a hundred larger than those reported here.

This large discrepancy is readily understood if we examine the approximations made by the Wright group. Their model for the Rydberg density assumes a single effective state with excitation cross section equal to 2.4×10^{-17} cm² and a radiative decay rate of 10^6 sec⁻¹ to give $\quad \sigma/A = 2.4 \times 10^{-23} \ (cf \ Eq. \ 2A),$ In our calculation the principal contribution to the excitation is to levels n=3, 4. For these states the contribution from $^1\Sigma_g, {}^1\Sigma_u, {}^1\Pi_u$ gives $\quad \sigma/A \simeq 2.2 \times 10^{-25} \quad$, and the factor of a hundred is recovered.

HIGH DENSITY SYSTEMS

Consider next the extrapolation to high-density, high-power systems. The relative contributions to the ion density are given by the relative values of the vibrational population and the Rydberg population, respectively. The vibrational population is equal, roughly speaking, to

$$N_2(v) = \frac{n_f \, N_2 \, \sigma v \, (E-V)}{[n_f \, \sigma v \, (e) + n_{th} \, \sigma v (diss)]} \left[1 - e^{-Dt}\right], \quad (11)$$

and the Rydberg population to

$$N_R(n) = \frac{n_f \, N_2 \, \sigma v \, (1-n)}{[A_n + n_{th} \, \sigma v \, (e)]} \left[1 - e^{-Dt}\right]. \quad (12)$$

Both expressions have the same density factors in the numerator. Both denominators are sensitive to the electron density, but the Rydberg denominator has a balance between excitation and radiative decay. Until the specific level or levels are known that express

the large dissociative attachment rates, the scaling with density is obscured by the radiative decay term. In the above it has been assumed that the large rates have their onset at n=3. If the onset is at n=5, for exmple, the ratio above for the FOM data is increased a factor of ten to five-hundred to one. But at n=5 the collisional term dominates the A_5 radiative term at electron densities a factor of four or more higher; and at these higher densities the ratio is again restored to approximately one hundred. The scaling of the ratio of the vibrational to Rydberg contributions with increased electron density will not be clarified precisely until the onset level for large dissociative attachment rates is known.

SUMMARY

The relative contributions of the high Rydberg states compared to the ground state vibrational excitation is of the order of one percent.
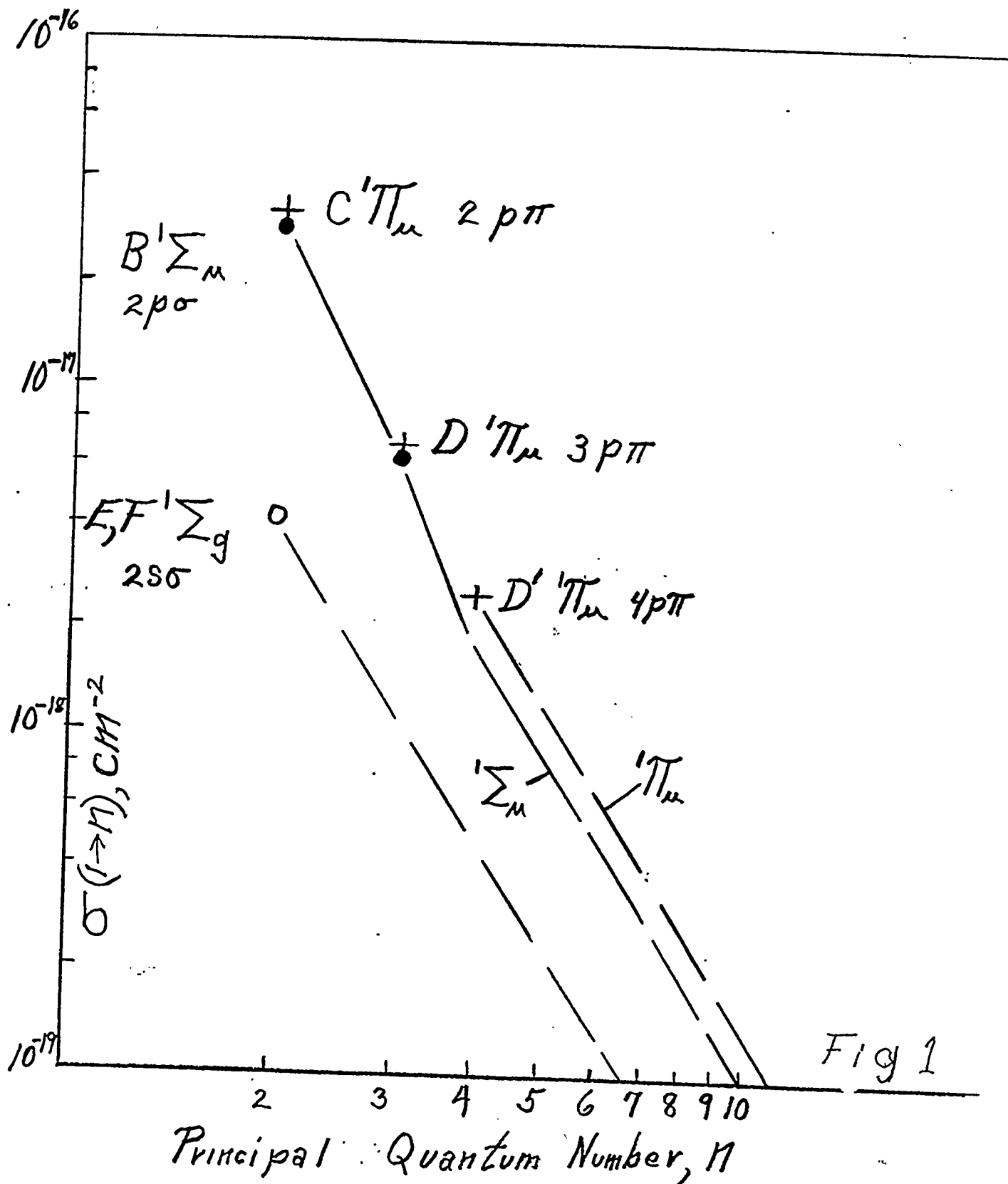
FIGURE CAPTIONS

Fig.1 Electron excitation rates versus parentage principal quantum number, n, for the $^1\Sigma_g$, $^1\Sigma_u$, and $^1\Pi_u$ sequences.

Fig.2 The radiative transition probabilities versus principal quantum number, n, for the $^1\Sigma_g$, $^1\Sigma_u$, and $^1\Pi_u$ sequences.

Fig.3 Rydberg populations, mol. cm^{-3} versus principal quantum number, n, for the lower limit and upper limit approximations.

Fig.4 Negative ion density versus discharge electron temperature: closed squares, Ref. 3; triangles, Refs. 8, 9; lower upper-lower limit symbols, these calculations; open circles, Ref. 10.
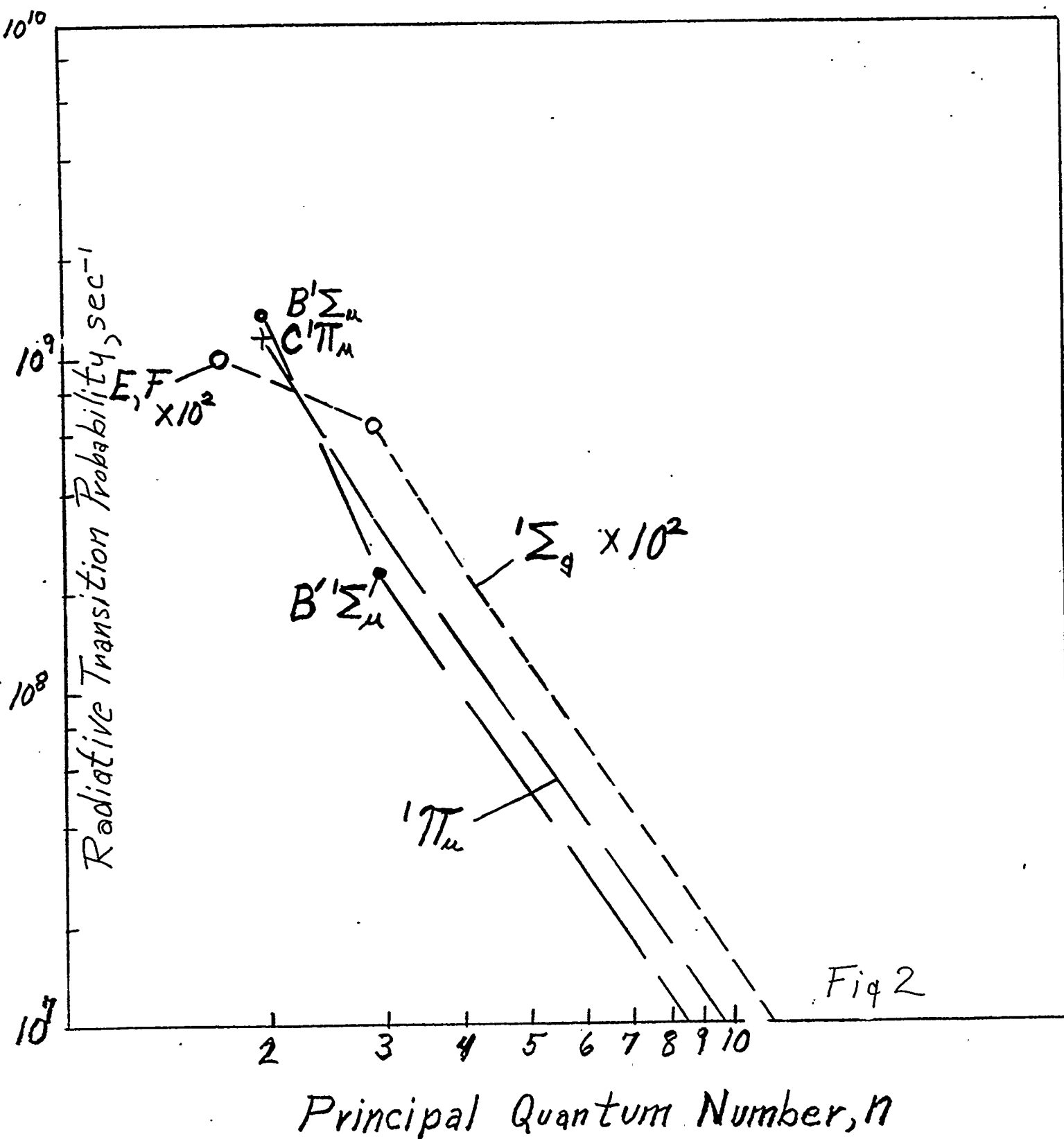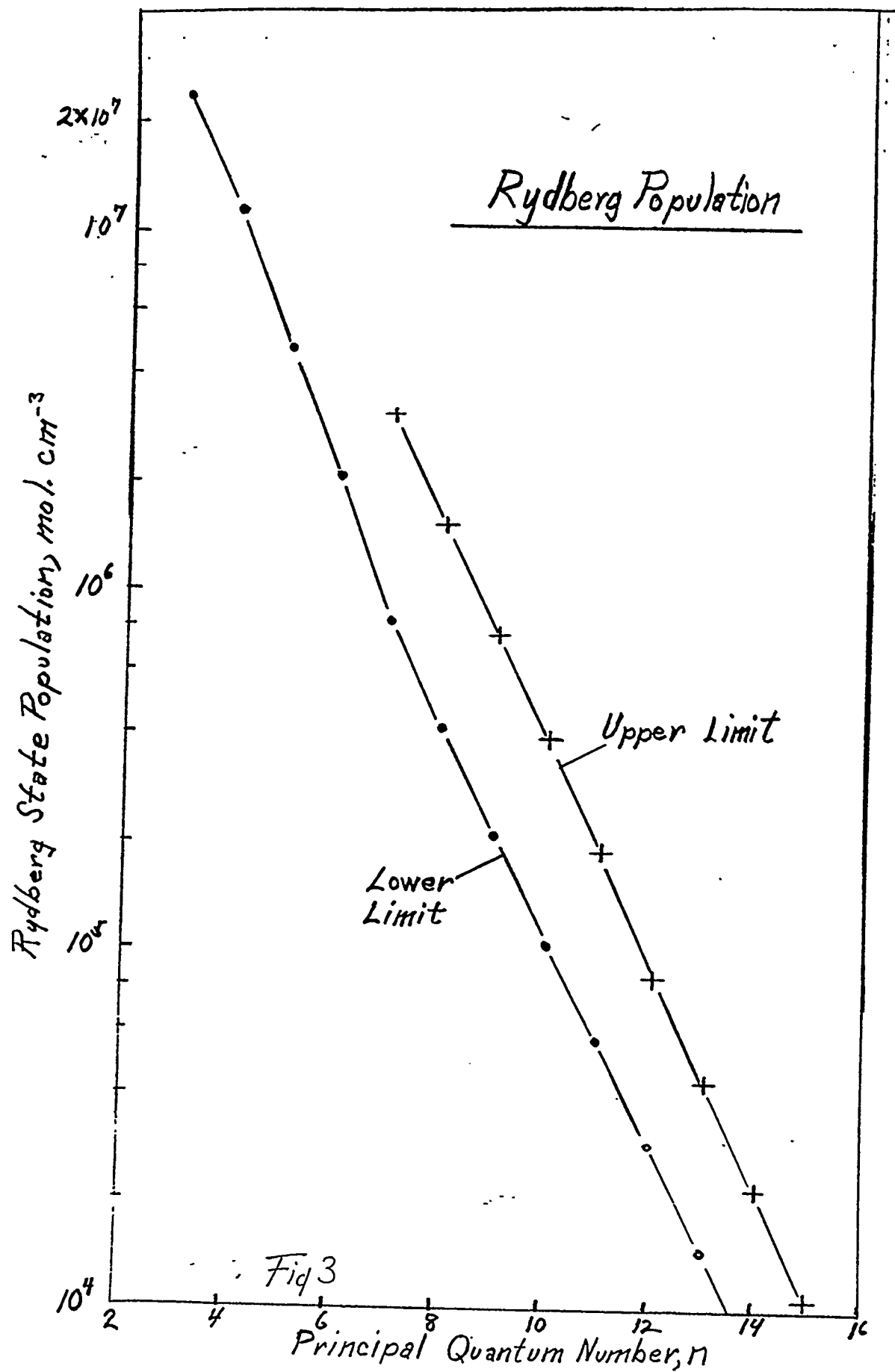
REFERENCES

1. L.A. Pinnaduwage and L.G. Christophorou, Phys. Rev. Lett. 70, 754 (1993).

2. L.A. Pinnaduwage and L.G. Christophorou, J. Appl. Phys. 76, 46 (1994).

3. P.J. Eenshuistra, R.M.A. Heeren, A.W. Kleyn, and H.J. Hopman, Phys. Rev. A40, 3613 (1989).

4. S. Rothenberg and E.R. Davidson, J. Mol. Spectrosc. 22, 1 (1967).

5. T.E. Sharp, Atomic Data, 2, 119 (1971).

6. J.R. Hiskes, Phys. Rev. Lett. 10. 102 (1963).

7. H.J. Hopman, Private Communication.

8. J.R. Hiskes, AIP Conf. Ser 287, p. 191, Nov. 1992.

9. J.R. Hiskes, to be published.

10. A. Garscadden and R. Nagpal, Plasma Sources Sci. Technol. 4, 268 (1995).

Excitation Cross Section $\sigma (1 \rightarrow n)$

Fig 1

Radiative Transition Probabilities, A_n

Fig 2

Rydberg Population

Upper Limit

Lower Limit

Fig 3

Rydberg State Population, mol. cm^{-3}

Principal Quantum Number, n

Fig 4

Legend:
- ● FOM - EXP.
- △ LLNL - $H_2(v)$ DA
- I LLNL - Rydberg DA
- O WRIGHT-Rydberg DA

Y-axis: 10^{11}, 10^{10}, 10^9

X-axis: Electron Temperature, eV (0.6, 0.8, 1.0, 1.2, 1.4)